

Structural changes of the choroid in sarcoid- and tuberculosis-related granulomatous uveitis

H Mehta¹, DA Sim^{2,3}, PA Keane^{2,3},
 J Zarranz-Ventura^{1,4}, K Gallagher¹, CA Egan¹,
 M Westcott¹, RWJ Lee^{1,2,3,5}, A Tufail^{1,2,3} and
 CE Pavesio^{1,2}

Abstract

Aim The aim of this study is to characterise the choroidal features of patients diagnosed with sarcoid- and tuberculosis (TB)-associated granulomatous uveitis using spectral domain optical coherence tomography (OCT).

Methods Twenty-seven patients (27 eyes) diagnosed with sarcoid- (13 eyes) and TB (14 eyes)-related uveitis were included in this retrospective, cross-sectional study. Over a six-month period, patients diagnosed with sarcoid and TB granulomatous uveitis were scanned using enhanced depth imaging OCT. Clinical and demographical characteristics were recorded, including the method of diagnosis, disease activity, site of inflammation (anterior or posterior), treatments, and visual acuity (VA). Manual segmentation of the choroidal layers was performed using custom image analysis software.

Results The main outcome measure was OCT-derived thickness measurements of the choroid and choroidal sublayers (Haller's large vessel and Sattler's medium vessel layers) at the macula region. The ratio of Haller's large vessel to Sattler's medium vessel layer was significantly different at the total macula circle in eyes diagnosed with TB uveitis (1.47 (= 140.71/95.72 μm)) compared with sarcoid uveitis (1.07 (= 137.70/128.69 μm)) ($P = 0.001$). A thinner choroid was observed in eyes with a VA ≥ 0.3 LogMAR (Snellen 6/12; 198.1 μm (interquartile range (IQR) = 147.0–253.4 μm) compared with those with VA < 0.3 LogMAR (292.4 μm (IQR = 240.1–347.6 μm)) at the total macula circle ($P = 0.004$). At the foveal central subfield, the median choroidal thickness was 336.8 μm (IQR = 272.3–375.4 μm) in active compared with 239.3 μm (IQR = 195.3–330.9 μm) in quiescent disease ($P = 0.04$).

Conclusion A disproportionately enlarged Sattler's layer may indicate a diagnosis of sarcoid-related uveitis, and choroidal

thickening may be a feature of active granulomatous uveitis.

Eye (2015) 29, 1060–1068; doi:10.1038/eye.2015.65;
 published online 29 May 2015

Introduction

Granulomatous uveitis is a chronic inflammatory process that can involve both the anterior and posterior segments of the eye.¹ It is characterised by clinical features including 'mutton-fat' keratic precipitates in the cornea, cells within the anterior chamber and vitreous, retinal vasculitis, and focal or diffuse choroidal lesions.^{2–5} Granulomatous disease may result from either an autoimmune process, most commonly sarcoidosis,^{2,3} or a systemic infection, usually tuberculosis (TB),^{2,6,7} occurring either as an isolated ocular condition or as part of a wider systemic disease.⁸

Sarcoid- and TB-associated granulomatous uveitis can cause visual disability from inflammatory sequelae such as cystoid macula oedema, glaucoma, or chorioretinal ischaemia.⁹ Fortunately, the majority of patients with sarcoid- and TB-associated uveitis are responsive to immunosuppressive treatment and/or the appropriate antimicrobial therapy.¹⁰ However, these treatments can have potential side effects, causing significant ocular and systemic morbidity linked to duration and dosage of treatment and even a possible increase in mortality rates with biologics such as TNF α .^{11,12} And so, the clinician faces the constant challenge of balancing the risk of uncontrolled inflammation on visual outcome with the potentially devastating side effects of immunosuppressive therapy. It is therefore important that the level of treatment for each individual patient is closely titrated against disease activity. In current practice, methods for assessing disease activity are largely reliant on

¹Medical Retina and Uveitis Service, Department of Ophthalmology, Moorfields Eye Hospital NHS Foundation Trust, London, UK

²NIHR Moorfields Biomedical Research Centre, London, UK

³Institute of Ophthalmology, University London, London, UK

⁴Vitreo-Retinal Service, Bristol Eye Hospital, Bristol, UK

⁵School of Clinical Sciences, University of Bristol, Bristol, UK

Correspondence: CE Pavesio, Medical Retina and Uveitis Service, Department of Ophthalmology, Moorfields Eye Hospital NHS Foundation Trust, 162 City Road, London EC1V 2PD, UK
 Tel: +44 (0)20 7894791061;
 Fax: +44 (0)20 75662972.
 E-mail: Carlos.Pavesio@moorfields.nhs.uk

Received: 17 June 2014
 Accepted in revised form: 21 March 2015
 Published online: 29 May 2015

clinical examination—grading the number of cells and intensity of flare in anterior chamber or vitreous by manual or automated means, or measuring the size of retinal or choroidal lesions.¹³ Although fluorescein and indocyanine green angiography offers additional information regarding disease activity, it is an invasive procedure, and not suitable for the frequent testing required to closely titrate treatment to disease activity in the patient.¹⁴

In recent years, the rapid advancement of optical coherence tomography (OCT) technology has allowed non-invasive imaging of the choroid in addition to the retina in cross-section.^{15–17} Several early studies have indicated how OCT-derived choroidal images can be useful in uveitic disorders. For example, OCT has been used (1) to describe characteristic features of specific uveitis entities, including thinning of Haller's large vessel layer of the choroid in idiopathic panuveitis and extra-macular choroidal changes in birdshot chorioretinopathy;^{18,19} (2) to identify distinct stages of a disease process as illustrated by punctate inner choroidopathy;^{20,21} (3) objective measurement of vitreous inflammation;²² and (4) to monitor response to therapy, exemplified by a reduction of subfoveal choroidal thickening with corticosteroid therapy in Vogt-Koyanagi-Harada disease.²³ Additionally, the potential of OCT angiography in uveitic diseases has yet to be realised.

In this study, we used enhanced depth imaging (EDI) protocols to acquire OCT-derived images of the choroid in eyes with sarcoid- and TB-associated granulomatous uveitis. Quantitative analysis of these images was performed in an effort to identify parameters, which may potentially be applied in the clinical arena, for example, to aid diagnosis and measure disease activity.

Materials and methods

Data collection

Clinical and imaging data from patients with granulomatous uveitis were collected retrospectively from consecutive patients attending Moorfields Eye Hospital uveitis clinics over the first 6 months of 2012. Patient notes were also checked 12 months later to confirm diagnoses. Approval for data collection and analysis was obtained from the Moorfields Eye Hospital research and ethics committee and adhered to the tenets set forth in the Declaration of Helsinki.

Diagnostic and inclusion criteria

The First International Workshop on Ocular Sarcoidosis (FIWOS) recommended four levels of certainty for diagnosis in patients in whom other possible causes of

uveitis had been excluded:²⁴ (1) biopsy-supported diagnosis with a compatible uveitis was labelled as definite ocular sarcoidosis; (2) if biopsy was not done but the chest X-ray was positive showing bihilar lymphadenopathy associated with a compatible uveitis, the condition was labelled as presumed ocular sarcoidosis; (3) if biopsy was not done and the chest X-ray did not show bihilar lymphadenopathy but there were three of the classic intraocular signs and two positive laboratory tests, the condition was labelled as probable ocular sarcoidosis; and (4) if lung biopsy was done and the result was negative but at least four classic intraocular signs and two positive laboratory investigations were present, the condition was labelled as possible ocular sarcoidosis. Only patients with definite, presumed or probable sarcoidosis were included in this study. The combination of clinical signs and laboratory tests proposed by the FIWOS has been validated to be highly specific and sensitive for the diagnosis of ocular sarcoidosis.²⁵

With TB-associated uveitis, the large variations in clinical presentation and the lack of uniformity in diagnostic criteria makes diagnosis difficult.²⁶ Most patients have no evidence of *Mycobacterium tuberculosis* in their ocular biopsies.²⁷ Patients with clinical ocular signs suggestive of TB,⁵ and positive microscopy or culture of *Mycobacterium tuberculosis* from any bodily fluid, in the absence of another identifiable cause for their uveitis were labelled as definite ocular TB. In the absence of confirmatory microbiology, when other identifiable causes of uveitis had been excluded, patients were labelled as presumed ocular TB only if they met all of the following three published criteria: (1) ocular signs suggestive of TB⁵; (2) positive QuantiFERON-TB Gold test^{28–32}; and (3) positive response to anti-tuberculous therapy.³³

Disease activity was recorded from notes based on clinical examination and investigations including macula OCT, fundus fluorescein, and indocyanine green angiography. Anterior chamber activity was graded by measuring the number of cells and intensity of flare. Posterior segment activity was based on the clinician's impression of significant vitritis, vasculitis, chorioretinitis, and papillitis. Cases of intermediate uveitis, posterior uveitis, and panuveitis were recorded as 'posterior uveitis'. Only cases of isolated anterior chamber activity with or without cystoid macula oedema were recorded as 'anterior uveitis'.

Protocol for image acquisition

Each patient was scanned using custom EDI protocols first described by Spaide *et al*.¹⁵ In each case, a macular centred scan was performed on one eye, and consisted of

seven OCT B-scans obtained in a 20×5 degree horizontal raster pattern; with each individual B-scan generated from 50 averaged scans.

Quantitative analysis of OCT images

For the generation of retinal and choroidal thickness maps, raw OCT data were exported from the Heidelberg Spectralis OCT system and imported into validated custom grading software (OCTOR) developed by Doheny Image Reading Center, Los Angeles, CA, USA.^{34,35} All OCT image sets contained a minimum of 13 B-scans distributed in a horizontal raster pattern overlying the area covered by the nine subfields of the Early Treatment Diabetic Retinopathy Study (ETDRS) grid. For each OCT image set, the inner and outer boundaries of both the retina and the choroid were manually segmented. All boundaries were drawn in accordance with a standard OCT grading protocol by a grader masked to patient identity, underlying diagnosis and disease activity.³⁶

The retinal space was defined as the space lying between the inner aspect of the internal limiting membrane and the outer border of the photoreceptor outer segments. The choroid was defined as the space between the outer border of the retinal pigment epithelium and choroidoscleral junction. The choroid was further subdivided into Haller's large vessel and Sattler's medium vessel layers. On OCT, the walls of blood vessels appear hyperreflective, and their lumens appear hyporefective. Haller's large vessel layer was defined as the outer choroid, consisting of large hypointense spaces representing large vascular luminal spaces (with luminal-to-vessel wall ratio $\geq 50\%$).³⁷ Sattler's medium vessel layer consisted of small- to medium-sized hypointense spaces, surrounded by hyperintense stroma (with a lumen-to-vessel wall ratio $< 50\%$), giving a mottled appearance on scans. This layer also included the choriocapillaris, which is not easily distinguishable with the current resolution of OCT images.^{38,39}

The foveal central subfield (FCS), in μm , corresponds to the ETDRS central subfield (area 9), and the total macular circle (TMC) corresponds to ETDRS areas 1–9.

Statistical analysis

Non-parametric analyses were used as histograms reveal that the distribution of data was skewed to the left. The χ^2 -test was used to assess categorical variables and, Mann–Whitney *U*-test and Spearman's rank correlation coefficient were applied to continuous variables.

Owing to multiple statistical comparisons, we applied a Sidak correction to adjust *P*-values to a more stringent value of $P \leq 0.004$ to allow for an experimental wide type

1 error of 10%. Less stringent $P < 0.05$ were also presented. Statistical analyses were performed using SPSS software version 16 (SPSS, Inc., Chicago, IL, USA).

Results

Over a 6-month period, 36 patients with a diagnosis of granulomatous uveitis suspected to be secondary to sarcoidosis or TB were imaged according to the protocol above. Nine patients were excluded as diagnoses were later reclassified (one syphilis, one Lyme disease, and seven idiopathic panuveitis). Patient demographics and clinical characteristics of the 27 patients included are listed in Table 1.

Baseline characteristics

The median age of all patients was 51 years (interquartile range (IQR) = 37–62, range = 20–80). The median age of patients diagnosed with sarcoidosis was 52 years (IQR = 45–63, range = 28–70), greater compared with patients with TB at 46 years (IQR = 36–58, range = 20–80). However, this did not reach statistical significance ($P = 0.20$). There was also no significant difference between visual acuity (VA), gender, diagnosis subtype, disease activity, and anatomical site of uveitis or treatment regimes between groups (Table 1).

The effects of granulomatous uveitis on choroidal morphology

Sattler's medium vessel layer of the choroid is thicker in eyes diagnosed with sarcoidosis The ratio of median Haller's large vessel layer to median Sattler's medium vessel layer was significantly different in eyes diagnosed with TB (1.47 (= 140.71/95.72 μm) compared with eyes diagnosed with sarcoidosis (1.07 (= 137.70/128.69 μm)) at the TMC ($P = 0.001$), but did not achieve statistical significance at the FCS (1.38 (= 162.85/118.01 μm) vs 1.15 (= 166.09/144.43 μm)) ($P = 0.02$; Figures 1 and 2). Most of the variation in choroidal thickness between sarcoid- and TB-related uveitis occurred in Sattler's medium vessel layer. No significant differences were observed in the choroidal sublayers between active or quiescent, or anterior or posterior disease. Although total choroidal thickness measurements were correlated with age at the TMC ($r = -0.51$, $P = 0.007$) and FCS ($r = -0.50$, $P = 0.007$), no associations between the ratio of median Haller's to median Sattler's vessel layers were observed at the TMC ($r = -0.23$, $P = 0.25$) and FCS ($r = -0.16$, $P = 0.44$).

VA and choroidal thickness measurements The median VA of all patients was 0.18 LogMAR (IQR = 0.00–0.30 LogMAR),

Table 1 Baseline demographic and clinical characteristics of patients diagnosed with sarcoidosis or tuberculosis

| | All patients (n = 27) | Sarcoidosis (n = 13) | Tuberculosis (n = 14) | P-value |
|------------------------------------|-----------------------|----------------------|-----------------------|---------|
| <i>Demographics</i> | | | | |
| Age, median (IQR) | 51 (37–62) | 52 (45–63) | 46 (36–58) | 0.20 |
| Female gender, n (%) | 16 (59.3) | 3 (23.1) | 8 (57.1) | 0.16 |
| Visual acuity—LogMAR, median (IQR) | 0.18 (0.00–0.30) | 0.18 (–0.08–0.18) | 0.24 (0.18–0.48) | 0.53 |
| <i>Diagnosis type, n (%)</i> | | | | |
| Presumed | 11 (40.7) | 4 (30.8) | 12 (85.7) | 0.08 |
| Probable | 4 (14.8) | 4 (30.8) | NA | |
| Definitive | 12 (44.4) | 5 (38.4) | 2 (14.3) | |
| <i>Disease activity, n (%)</i> | | | | |
| Active | 10 (37.0) | 5 (38.5) | 5 (35.7) | 0.80 |
| Quiescent | 17 (63.0) | 8 (61.5) | 9 (64.3) | |
| <i>Uveitis, n (%)</i> | | | | |
| Anterior | 5 (18.5) | 3 (23.1) | 2 (12.3) | 0.93 |
| Posterior | 22 (81.5) | 10 (76.9) | 12 (85.7) | |
| <i>Treatment</i> | | | | |
| Topical steroid, n (%) | 21 (77.7) | 10 (76.9) | 11 (78.6) | 0.88 |
| Oral steroids, n (%) | 11 (40.7) | 4 (30.8) | 7 (50.0) | 0.81 |
| Second-line agent, n (%) | 3 (11.1) | 2 (15.4) | 1 (7.1) | 0.88 |

Abbreviation: IQR, interquartile range.

and there was no difference between eyes diagnosed with TB or sarcoid (Table 1). However, in the TMC, eyes with a VA equal to, or worse than, 0.3 LogMAR had a significantly thinner choroid (198.1 μm (IQR = 147.0–253.4 μm)) compared with eyes with a VA better than 0.3 LogMAR (292.4 μm (IQR = 240.1–347.6 μm)) ($P=0.004$) with factors including age and disease activity well matched between these subgroups. However, at the FCS, this did not reach statistical significance ($P=0.02$; Figure 3). Choroidal thickness measurements, showed a modest correlation with LogMAR VA ($R^2=-0.17$, $P=0.04$) at the TMC and FCS ($R^2=-0.10$, $P=0.10$), but did not reach statistical significance. There was no significant difference in age of the good VA (<0.3 LogMAR) group vs the poor VA (≥ 0.3 LogMAR) group ($P=0.27$).

The choroid in active and quiescent granulomatous uveitis The median choroidal thickness in all eyes was 262.4 μm (IQR = 202.6–299.2 μm) at the TMC, and 287.4 μm (IQR = 216.6–343.3 μm) at the FCS. At the FCS, the choroid appeared thicker in eyes with active (336.8 μm (IQR = 272.3–375.4 μm)) compared with quiescent granulomatous uveitis (239.3 μm (IQR = 195.3–330.9 μm)), but this failed to reach statistical significance at the stringent 0.004 level ($P=0.04$; Figures 1 and 3). There were no significant difference in age between active and quiescent groups ($P=0.50$).

The effects of granulomatous uveitis on retinal morphology

In the 27 eyes analysed, the median retinal thickness measurement was 286.5 μm (IQR = 271.2–309.1 μm) at the TMC and 235.9 μm (IQR = 216.6–261.7 μm) at the FCS. Retinal thickness measurements at the TMC and FCS showed good correlation within patients ($R^2=0.56$, $P=0.0001$). There were no significant differences in retinal thickness between type of granulomatous uveitis, disease activity or anatomical site of uveitis.

Discussion

In this cross-sectional study, we assessed OCT-derived measurements of choroidal thickness, and its component Haller’s large and Sattler’s medium vessel layers, in eyes with sarcoid- and TB-associated granulomatous uveitis.

The ratio of Haller’s large to Sattler’s medium vessel layer measured over the TMC was significantly different in eyes with sarcoid compared with TB uveitis. Although the median total choroidal thickness measurements were not different between both entities, Sattler’s medium vessel layer on average contributed 48.3% of the total macular choroidal thickness in sarcoid uveitis compared with 40.5% in TB uveitis. However, there was no distinct cutoff in the ratio of these layers to reliably distinguish between these granulomatous diseases. A published data

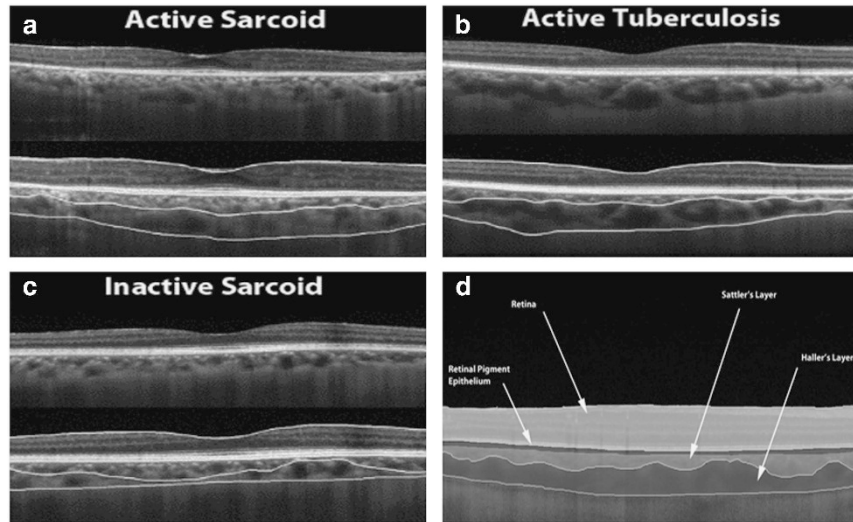


Figure 1 EDI-OCT images of the choroid in (a) active sarcoidosis, (b) active tuberculosis, and (c) inactive sarcoidosis. (d) Demonstrates the retina, retinal pigment epithelium, and Haller's large and Sattler's medium vessel choroidal layers. Although the median total choroidal thickness measurements were not different between sarcoid and TB uveitis groups, the ratio of median Haller's large to median Sattler's medium vessel layers at the total macula circle was significantly different in eyes diagnosed with TB (1.47 (= 140.71 μm/95.72 μm)) compared to eyes diagnosed with sarcoidosis (1.07 (= 137.70 μm/128.69 μm)) ($P=0.001$). At the foveal central subfield, the choroid was thicker in eyes with active (336.8 μm (IQR = 272.3–375.4 μm)) compared with inactive granulomatous uveitis (239.3 μm (IQR = 195.3–330.9 μm)) but this failed to reach statistical significance at the stringent 0.004 level ($P=0.04$).

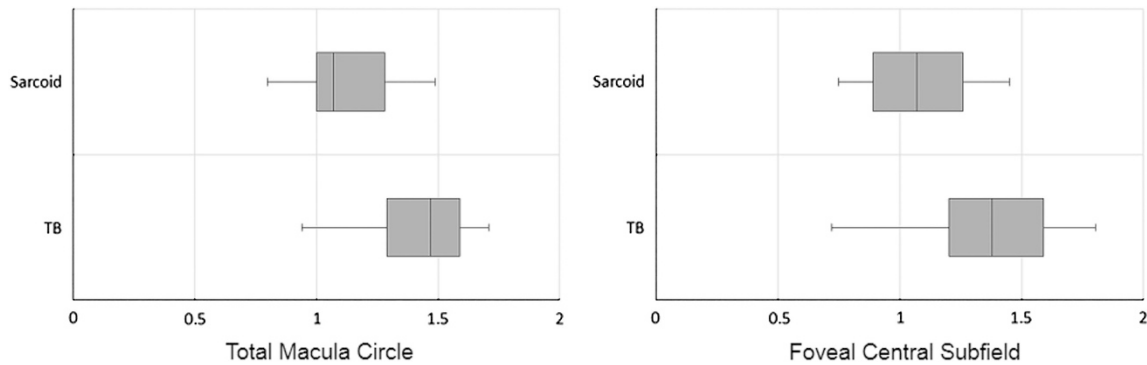


Figure 2 Box plot of ratio of Haller's to Sattler's choroidal sublayers in eyes diagnosed with TB compared with sarcoid uveitis. This box plot demonstrates that the ratio of median Haller's large to median Sattler's medium vessel layers at the total macula circle was significantly different in eyes diagnosed with TB (1.47 (= 140.71/95.72 μm)) compared with eyes diagnosed with sarcoidosis (1.07 (= 137.70/128.69 μm)) ($P=0.001$). Sattler's medium vessel layer was disproportionately enlarged in eyes diagnosed with sarcoid compared with TB uveitis. This did not achieve statistical significant at the FCS (1.38 (= 162.85/118.01 μm) for TB vs 1.15 (= 166.09/144.43 μm) for sarcoid) ($P=0.02$). There was also no distinct cutoff in the ratio of these layers to reliably distinguish between the diseases. Quartiles 1 and 3 are delineated by the borders of the box. The median is represented by the solid line within the box. The whiskers extend from quartile 1 to the minimum value and from quartile 3 to the maximum value. Because of the skew of the data, medians and IQRs were presented.

set of healthy subjects reported that Sattler's layer contributed ~20–30% of the macular choroidal thickness.³⁹

We speculate that the difference in relative thickness of the choroidal sublayers may reflect the different underlying pathogenesis of sarcoid- and TB-related

uveitis. In 1976, Gass and Olson⁴⁰ in a clinicopathological correlative study of a patient with sarcoid posterior uveitis, found that lesions labelled as 'focal choroiditis' were actually below the retinal pigment epithelium and not within the choroid. Other studies have since supported these findings, observing that in

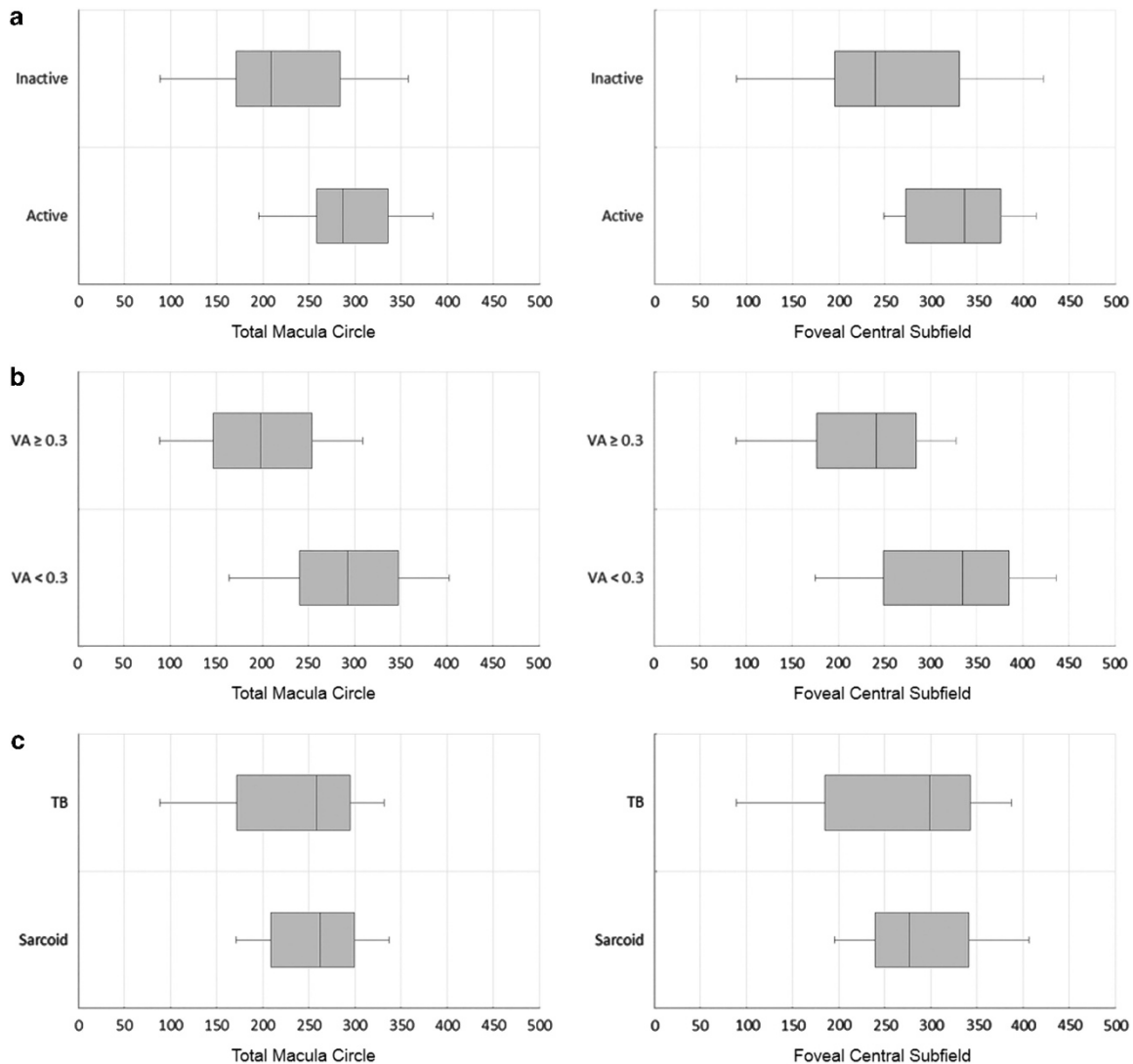


Figure 3 Box plots of choroidal thickness measurements in eyes with granulomatous uveitis secondary to sarcoidosis or TB. These box plots demonstrate the distribution of choroidal thicknesses for the TMC and FCS according to (a) disease activity, (b) good (<0.3 LogMAR) or poor (≥ 0.3 LogMAR) VA, and (c) diagnosis of TB or sarcoid uveitis. (a) At the FCS, the choroid was thicker in eyes with active ($336.8 \mu\text{m}$ (IQR = 272.3 – $375.4 \mu\text{m}$)) compared with quiescent granulomatous uveitis ($239.3 \mu\text{m}$ (IQR = 195.3 – $330.9 \mu\text{m}$)), but this failed to reach statistical significance at the stringent 0.004 level ($P=0.04$). (b) In the TMC, eyes with a VA ≥ 0.3 LogMAR had a significantly thinner choroid ($198.1 \mu\text{m}$ (IQR = 147.0 – $253.4 \mu\text{m}$)) compared with eyes with a VA < 0.3 LogMAR ($292.4 \mu\text{m}$ (IQR = 240.1 – $347.6 \mu\text{m}$)) ($P=0.004$) with factors including age and disease activity well matched between these subgroups. However, at the FCS, this did not reach statistical significance ($P=0.02$). (c) Total choroidal thickness was not helpful in distinguishing between TB and sarcoid uveitis at the TMC ($P=0.26$) or FCS ($P=0.69$).

sarcoid-associated uveitis, deep choroidal involvement is infrequent.^{41,42} This is in contrast to TB-associated uveitis where choroidal involvement is commonly observed.^{4,43} Furthermore, in a recent clinical study, it was observed that ocular TB in the posterior segment presents as a retinal vasculitis that not only predominantly affects venous structures but also chorioretinal structures adjacent to involved vessels. In comparison, the classic feature of sarcoid-associated posterior uveitis, ‘candle wax drippings’, was found to

be a periphlebitis primarily located in the inferior retinal periphery without adjacent vascular or choroidal involvement.⁸ If future prospective studies confirm that the relative thickness of the sublayers of the choroid are indeed characteristic for either disease, EDI-OCT may prove a useful aid in the diagnosis of these granulomatous diseases. It should be noted that TB-associated uveitis can have disparate retinal and choroidal manifestations, and this study, with the relatively few cases available, cannot distinguish

whether there are differences in choroidal thickness measurements according to the type of presentation.

In this study, we observed an association between a thin choroid and poor VA at the TMC ($P=0.004$), but interestingly not the same degree of significance at the FCS ($P=0.02$). A possible explanation is that OCT images over the TMC cover a larger area ($9\pi \text{ mm}^2$) than the FCS ($0.25\pi \text{ mm}^2$), and therefore the TMC is more representative of the total choroidal thickness of the eye. It may be that occurrence of choroidal inflammation over extended periods ultimately leads to generalised choroidal atrophy and thinning, and it is this, rather than focal choroidal atrophy under the fovea, that affects visual function. This raises the question as to whether choroidal thinning in chronic granulomatous disease is localised to the macula region or more widespread, especially as granulomatous uveitis can present with diffuse posterior segment signs.^{5,42,44} In a recent study, extra-macular scans performed in eyes diagnosed with birdshot chorioretinitis demonstrated generalised choroidal thinning outside the macula.¹⁸ Although factors including age and disease activity were well matched between the good (<0.3 LogMAR) and poor (≥ 0.3 LogMAR) VA groups, other confounders are possible.

EDI-OCT studies into other uveitic conditions such as Vogt-Koyanagi-Harada disease²³ and Behçet's disease⁴⁵ have observed a thicker choroid in active compared with quiescent disease. A possible explanation for this observation is that in the presence of inflammation, the release of mediators such as prostaglandins causes blood vessels to dilate leading to increases in OCT-derived measurements of choroidal thickness.⁴⁶ This does not occur in the vessels of the retina as autoregulation maintains a constant perfusion pressure to the corresponding vascular tree.⁴⁷ However, in the highly vascular choroid, no such autoregulatory mechanism is present.^{48,49} We hypothesise that the 'spongiform' choroidal vasculature is highly reactive to changes in the inflammatory state of the immediate environment, with consequent changes to choroidal thickness measurements. Measuring choroidal thickness could therefore provide a non-invasive method to monitor disease activity within an individual over time. This would be important in addressing the difficult therapeutic question encountered in clinical practice—when and how quickly to taper immunosuppressive therapy, thereby allowing treatment to be better tailored to the individual patient.

In this cross-sectional study, we observed a trend of a thicker choroid in active (median $336.8 \mu\text{m}$ (IQR = 272.3 – $375.4 \mu\text{m}$)) compared with quiescent (median $239.3 \mu\text{m}$ (IQR = 195.3 – $330.9 \mu\text{m}$)) granulomatous uveitis ($P=0.04$), but this did not reach statistical significance at the stringent $P \leq 0.004$ level set to avoid the chance of type 1 errors. This might be explained by the observation that

choroidal thickness is highly variable between individuals and is significantly dependent on variables such as age and sex, which were recorded in this study, and factors such as refractive error and axial length, which were not recorded. However, looking for longitudinal changes within an individual may allow some of the natural choroidal variation between individuals to be accounted for.^{50–53}

Strengths of the study included the use of a validated segmentation protocol to analyse OCT images from patients with a relatively rare disease entity.³⁶ To the authors' knowledge, this is the largest EDI-OCT study in granulomatous uveitis to date. There are a number of limitations. First, it included patients from a single tertiary referral centre that has a bias towards a more severe spectrum of disease. However, the data presented are likely to represent the patient cohort more likely to require immunosuppressive therapy and hence close monitoring. Second, the retrospective cross-sectional design carries inherent bias and longitudinal prospective studies involving larger patient cohorts and dual-grading will be required to confirm our findings. Third, diagnoses were not all based on biopsy-proven cases. This reflects real world clinical practice. The clinical and laboratory diagnostic criteria, detailed in the Materials and methods section, has high specificity and sensitivity reported in the published literature.^{25,28} Fourth, imaging with current OCT equipment was limited to the macula region, and as discussed above preliminary evidence suggests that extra-macular scans may be more discriminatory for disease activity and visual function. It is likely that next-generation OCT devices, with faster acquisition times, will allow larger areas of the choroid to be assessed.⁵⁴ Finally, we used manual segmentation using custom software that is not currently available in the clinical arena. However, efforts are underway to provide automated choroidal thickness maps, similar to automated retinal thickness maps currently available, particularly with the coming next-generation OCT systems.⁵⁵

In conclusion, we observed that Sattler's medium vessel layer was disproportionately enlarged in sarcoid compared with TB-related uveitis, and there is a trend for the choroid to be thicker in active granulomatous uveitis. In addition, choroidal thinning was observed to be associated with reduced VA. These OCT-derived parameters of the choroid, if validated in larger prospective studies, may not only offer insights into diagnosis and visual prognosis for eyes with granulomatous uveitis but also potentially be used to monitor disease activity within an individual over time or as an objective measure for clinical trials.

Summary

What was known before

- Enhanced depth optical coherence tomography (OCT) imaging of the choroid has offered insights into uveitis, namely (1) description of characteristic features of specific uveitis entities, including extra-macular choroidal changes in birdshot chorioretinopathy; (2) identification of distinct stages of a disease process as illustrated by punctate inner choroidopathy; and (3) monitoring response to therapy, exemplified by a reduction of subfoveal choroidal thickening with corticosteroid therapy in Vogt-Koyanagi-Harada disease. This study assesses the structural characteristics of the choroid in granulomatous uveitis using OCT imaging.

What this study adds

- OCT-derived parameters of the choroid offer insights into the underlying diagnosis and disease activity in granulomatous uveitis. Sattler's medium-sized vessel choroidal layer appears disproportionately enlarged in sarcoid compared with tuberculosis uveitis. The choroid appears to be thicker in active granulomatous uveitis.

Conflict of interest

The authors declare no conflict of interest.

Acknowledgements

DAS receives funding from Fight For Sight UK, Grant 1987. DAS, PAK and JZ-V have received travel grants from the Allergan European Retina Panel. JZ-V is a grant recipient of the Spanish Retina and Vitreous Society (Sociedad Española de Retina y Vítreo, SERV). DAS, PAK, CAE, AT and CEP have received a proportion of their funding from the Department of Health's NIHR Biomedical Research Centre for Ophthalmology at Moorfields Eye Hospital and UCL Institute of Ophthalmology. The views expressed in the publication are those of the author and not necessarily those of the Department of Health.

References

- Marcus EI, Do DV, Shah SM, Nguyen QD, Biswas J, Levinson R. Diagnostic and therapeutic challenges. Granulomatous panuveitis. *Retina* 2008; **28**: 1544–1549.
- Jones NP. Sarcoidosis and uveitis. *Ophthalmol Clin North Am* 2002; **15**: 319–326 vi.
- Iannuzzi MC, Rybicki BA, Teirstein AS. Sarcoidosis. *N Engl J Med* 2007; **357**: 2153–2165.
- Massaro D, Katz S, Sachs M. Choroidal tubercles. A clue to hematogenous tuberculosis. *Ann Int Med* 1964; **60**: 231–241.
- Gupta A, Bansal R, Gupta V, Sharma A, Bamberg P. Ocular signs predictive of tubercular uveitis. *Am J Ophthalmol* 2010; **149**: 562–570.
- Gupta V, Gupta A, Rao NA. Intraocular tuberculosis—an update. *Surv Ophthalmol* 2007; **52**: 561–587.
- Yeh S, Sen HN, Colyer M, Zapor M, Wroblewski K. Update on ocular tuberculosis. *Curr Opin Ophthalmol* 2012; **23**: 551–556.
- Babu K, Kini R, Mehta R, Philips M, Subbakrishna DK, Murthy KR. Predictors for tubercular uveitis: a comparison between biopsy-proven cases of tubercular and sarcoid uveitis. *Retina* 2012; **32**: 1017–1020.
- Miserocchi E, Modorati G, Di Matteo F, Galli L, Rama P, Bandello F. Visual outcome in ocular sarcoidosis: retrospective evaluation of risk factors. *Eur J Ophthalmol* 2011; **21**: 802–810.
- Manousaridis K, Ong E, Stenton C, Gupta R, Browning AC, Pandit R. Clinical presentation, treatment, and outcomes in presumed intraocular tuberculosis: experience from Newcastle upon Tyne, UK. *Eye (Lond)* 2013; **27**: 480–486.
- Imrie FR, Dick AD. Biologics in the treatment of uveitis. *Curr Opin Ophthalmol* 2007; **18**: 481–486.
- Kempen JH, Daniel E, Dunn JP, Foster CS, Gangaputra S, Hanish A et al. Overall and cancer related mortality among patients with ocular inflammation treated with immunosuppressive drugs: retrospective cohort study. *BMJ* 2009; **339**: b2480.
- Herbert CP, Tugal-Tutkun I. Editorial: Laser flare (cell) photometry: 20 years already. *Int Ophthalmol* 2010; **30**: 445–447.
- Herbert CP. Fluorescein and indocyanine green angiography for uveitis. *Middle East Afr J Ophthalmol* 2009; **16**: 168–187.
- Spaide RF, Koizumi H, Pozzoni MC. Enhanced depth imaging spectral-domain optical coherence tomography. *Am J Ophthalmol* 2008; **146**: 496–500.
- Ouyang Y, Heussen FM, Mokwa N, Walsh AC, Durbin MK, Keane PA et al. Spatial distribution of posterior pole choroidal thickness by spectral domain optical coherence tomography. *Invest Ophthalmol Vis Sci* 2011; **52**: 7019–7026.
- Margolis R, Spaide RF. A pilot study of enhanced depth imaging optical coherence tomography of the choroid in normal eyes. *Am J Ophthalmol* 2009; **147**: 811–815.
- Keane PA, Allie M, Turner SJ, Southworth HS, Sadda SR, Murray PI et al. Characterization of birdshot chorioretinopathy using extramacular enhanced depth optical coherence tomography. *JAMA Ophthalmol* 2013; **131**: 341–350.
- Karampelas M, Sim DA, Keane PA, Zarranz-Ventura J, Patel PJ, Tufail A et al. Choroidal assessment in idiopathic panuveitis using optical coherence tomography. *Graefes Arch Clin Exp Ophthalmol* 2013; **251**: 2029–2036.
- Zhang X, Zuo C, Li M, Chen H, Huang S, Wen F. Spectral-domain optical coherence tomographic findings at each stage of punctate inner choroidopathy. *Ophthalmology* 2013; **120**: 2678–2683.
- Zarranz-Ventura J, Sim DA, Keane PA, Patel PJ, Westcott MC, Lee RW et al. Characterization of Punctate Inner Choroidopathy Using Enhanced Depth Imaging Optical Coherence Tomography. *Ophthalmology* 2014; **121**: 1790–1797.
- Keane PA, Karampelas M, Sim DA, Sadda SR, Tufail A, Sen HN et al. Objective measurement of vitreous inflammation using optical coherence tomography. *Ophthalmology* 2014; **121**: 1706–1714.
- Nakayama M, Keino H, Okada AA, Watanabe T, Taki W, Inoue M et al. Enhanced depth imaging optical coherence tomography of the choroid in Vogt-Koyanagi-Harada disease. *Retina* 2012; **32**: 2061–2069.

- 24 Herbot CP, Rao NA, Mochizuki M. International criteria for the diagnosis of ocular sarcoidosis: results of the first International Workshop On Ocular Sarcoidosis (IWOS). *Ocul Immunol Inflamm* 2009; **17**: 160–169.
- 25 Takase H, Shimizu K, Yamada Y, Hanada A, Takahashi H, Mochizuki M. Validation of international criteria for the diagnosis of ocular sarcoidosis proposed by the first international workshop on ocular sarcoidosis. *Jpn J Ophthalmol* 2010; **54**: 529–536.
- 26 Cunningham ET, Rathinam SR. TB or not TB? The perennial question. *Br J Ophthalmol* 2001; **85**: 127–128.
- 27 Ang M, Cheung G, Vania M, Chen J, Yang H, Li J, Chee SP. Aqueous cytokine and chemokine analysis in uveitis associated with tuberculosis. *Mol Vis* 2012; **18**: 565–573.
- 28 Ang M, Wong WL, Li X, Chee SP. Interferon gamma release assay for the diagnosis of uveitis associated with tuberculosis: a Bayesian evaluation in the absence of a gold standard. *Br J Ophthalmol* 2013; **97**: 1062–1067.
- 29 Itty S, Bakri SJ, Pulido JS, Herman DC, Faia LJ, Tufty GT et al. Initial results of QuantiFERON-TB Gold testing in patients with uveitis. *Eye (Lond)* 2009; **23**: 904–909.
- 30 Mackensen F, Becker MD, Wiehler U, Max R, Dalpke A, Zimmermann S. QuantiFERON TB-Gold—a new test strengthening long-suspected tuberculous involvement in serpiginous-like choroiditis. *Am J Ophthalmol* 2008; **146**: 761–766.
- 31 La Distia Nora R, van Velthoven ME, Ten Dam-van Loon NH, Misotten T, Bakker M, van Hagen MP et al. Clinical manifestations of patients with intraocular inflammation and positive QuantiFERON-TB gold in-tube test in a country nonendemic for tuberculosis. *Am J Ophthalmol* 2014; **157**: 754–761.
- 32 Pepple KL, Van Gelder R, Forooghian F. Caveats about QuantiFERON-TB gold in-tube testing for uveitis. *Am J Ophthalmol* 2014; **157**: 752–753.
- 33 Ang M, Htoon HM, Chee SP. Diagnosis of tuberculous uveitis: clinical application of an interferon-gamma release assay. *Ophthalmology* 2009; **116**: 1391–1396.
- 34 Sadda SR, Keane PA, Ouyang Y, Updike JF, Walsh AC. Impact of scanning density on measurements from spectral domain optical coherence tomography. *Invest Ophthalmol Vis Sci* 2010; **51**: 1071–1078.
- 35 Sadda SR, Joeres S, Wu Z, Updike P, Romano P, Collins AT et al. Error correction and quantitative subanalysis of optical coherence tomography data using computer-assisted grading. *Invest Ophthalmol Vis Sci* 2007; **48**: 839–848.
- 36 Joeres S, Tsong JW, Updike PG, Collins AT, Dustin L, Walsh AC et al. Reproducibility of quantitative optical coherence tomography subanalysis in neovascular age-related macular degeneration. *Invest Ophthalmol Vis Sci* 2007; **48**: 4300–4307.
- 37 Adhi M, Lau M, Liang MC, Waheed NK, Duker JS. Analysis of the thickness and vascular layers of the choroid in eyes with geographic atrophy using spectral-domain optical coherence tomography. *Retina* 2014; **34**: 306–312.
- 38 Sim DA, Keane PA, Mehta H, Fung S, Zarranz-Ventura J, Fruttiger M et al. Repeatability and reproducibility of choroidal vessel layer measurements in diabetic retinopathy using enhanced depth optical coherence tomography. *Invest Ophthalmol Vis Sci* 2013; **54**: 2893–2901.
- 39 Branchini LA, Adhi M, Regatieri CV, Nandakumar N, Liu JJ, Laver N et al. Analysis of choroidal morphologic features and vasculature in healthy eyes using spectral-domain optical coherence tomography. *Ophthalmology* 2013; **120**: 1901–1908.
- 40 Gass JD, Olson CL. Sarcoidosis with optic nerve and retinal involvement. *Arch Ophthalmol* 1976; **94**: 945–950.
- 41 Campo RV, Aaberg TM. Choroidal granuloma in sarcoidosis. *Am J Ophthalmol* 1984; **97**: 419–427.
- 42 Spalton DJ, Sanders MD. Fundus changes in histologically confirmed sarcoidosis. *Br J Ophthalmol* 1981; **65**: 348–358.
- 43 Demirci H, Shields CL, Shields JA, Eagle RC Jr. Ocular tuberculosis masquerading as ocular tumors. *Surv Ophthalmol* 2004; **49**: 78–89.
- 44 Gungor SG, Akkoyun I, Reyhan NH, Yesilirmak N, Yilmaz G. Choroidal thickness in ocular sarcoidosis during quiescent phase using enhanced depth imaging optical coherence tomography. *Ocul Immunol Inflamm* 2014; **22**(4): 287–293.
- 45 Kim M, Kim H, Kwon HJ, Kim SS, Koh HJ, Lee SC. Choroidal thickness in Behcet's uveitis: an enhanced depth imaging-optical coherence tomography and its association with angiographic changes. *Invest Ophthalmol Vis Sci* 2013; **54**: 6033–6039.
- 46 Williams TJ. Oedema and vasodilatation in inflammation: the relevance of prostaglandins. *Postgrad Med J* 1977; **53**: 660–662.
- 47 Rassam SM, Patel V, Chen HC, Kohner EM. Regional retinal blood flow and vascular autoregulation. *Eye (Lond)* 1996; **10** (Pt 3): 331–337.
- 48 Bill A, Sperber GO. Control of retinal and choroidal blood flow. *Eye (Lond)* 1990; **4**(Pt 2): 319–325.
- 49 Weiter JJ, Ernest JT. Anatomy of the choroidal vasculature. *Am J Ophthalmol* 1974; **78**: 583–590.
- 50 Rahman W, Chen FK, Yeoh J, Patel P, Tufail A, Da Cruz L. Repeatability of manual subfoveal choroidal thickness measurements in healthy subjects using the technique of enhanced depth imaging optical coherence tomography. *Invest Ophthalmol Vis Sci* 2011; **52**: 2267–2271.
- 51 Li XQ, Larsen M, Munch IC. Subfoveal choroidal thickness in relation to sex and axial length in 93 Danish university students. *Invest Ophthalmol Vis Sci* 2011; **52**: 8438–8441.
- 52 Tan CS, Ouyang Y, Ruiz H, Sadda SR. Diurnal variation of choroidal thickness in normal, healthy subjects measured by spectral domain optical coherence tomography. *Invest Ophthalmol Vis Sci* **53**: 261–266.
- 53 Flores-Moreno I, Lugo F, Duker JS, Ruiz-Moreno JM. The relationship between axial length and choroidal thickness in eyes with high myopia. *Am J Ophthalmol* 2013; **155**: 314–319 e311.
- 54 Mrejen S, Spaide RF. Optical coherence tomography: Imaging of the choroid and beyond. *Surv Ophthalmol* 2013; **58**: 387–429.
- 55 Adhi M, Duker JS. Optical coherence tomography—current and future applications. *Curr Opin Ophthalmol* 2013; **24**: 213–221.